Am J Cancer Res 2023;13(6):2376-2391
www.ajcr.us /ISSN:2156-6976/ajcr0149056

Original Article

CKAP2 promotes cervical cancer progression by modulating the tumor microenvironment via NF-κB signaling

Luopei Guo[1*], Chunbo Li[1*], Jingjing Guo[1], Junjun Qiu[1], Keqin Hua[1,2]

[1]Obstetrics and Gynecology Hospital of Fudan University, Shanghai, China; [2]Shanghai Key Laboratory of Female Reproductive Endocrine Related Diseases, Shanghai, China. [*]Equal contributors.

Received January 10, 2023; Accepted May 6, 2023; Epub June 15, 2023; Published June 30, 2023

Abstract: This study aimed to investigate whether CKAP2 could promote cervical cancer (CC) progression by modulating the tumor microenvironment (TME) via NF-κB signaling. The communication between cervical cancer cells and the TME, including THP-1 and HUVECs, was tested. Gain- and loss-of-function assays were performed to elucidate the role of CKAP2 in cervical cancer progression. Western blot analysis was exploited to investigate the potential involved mechanism involved. Here, we reported that cervical cancer tissues were enriched with macrophages and microvessels. CKAP2 increased the tumor-promoting macrophage population. The overexpression of CKAP2 not only promoted endothelial cell viability and tube formation but also increased vascular permeability, and vice versa. Moreover, CKAP2 promoted cervical cancer progression via NF-κB signaling. This effect could be blocked by the NF-κB signaling inhibitor JSH-23. Our findings indicated that CKAP2 could promote cervical cancer progression by modulating the TME via NF-κB signaling.

Keywords: Tumor microenvironment, TAM, angiogenesis, CKAP2, metastasis, HUVEC

Introduction

Cervical Cancer is a common gynecological malignancy that does great harm to women's health and social hygiene. However, despite decades of extensive research, the mechanism of cervical cancer is still unknown. Recently, the TME has attracted considerable attention and has become a hot issue. Angiogenesis and immune regulation of the regional TME play essential roles in cervical cancer progression.

Tumor-associated macrophages (TAMs) are among the most abundant stromal cells in the cervical cancer microenvironment and have long been discussed. TAMs tend to present a more alternative M2-type characteristic, which promotes inflammation and tumor progression. A study revealing the relationship between TAMs and cervical intraepithelial neoplasia (CIN) was first published in 2007 [1]. Subsequently, an increasing number of reports showed that TAMs were positively correlated with cervical cancer, and could significantly help sustain a tumor immunosuppressive microenvironment and promote angiogenesis and metastasis [2]. Moreover, a previous study also discovered that cervical cancer conditioned medium (CM) may influence macrophage differentiation and further contribute to cervical cancer [3]. In addition, we systematically analyzed the TME and cervical cancer prognosis from TCGA. The cluster analysis uncovered 3 distinct patterns of TME subtypes with clinicopathologic features, including Clusters A, B and C. And TME Cluster B was characterized by highest infiltrative levels of macrophages and showed worst prognosis. Therefore, we particularly focused on macrophages in this study.

Angiogenesis is essential to the TME, and the formation of angiogenesis from preexisting blood vessels provides rich nutrition for tumor growth; therefore, anti-angiogenesis treatments occupy an important place in cancer therapy. Under hypoxic conditions, inflammatory cells are recruited, vascular growth factors are produced, the basement membrane is

degraded, and endothelial cells migrate, proliferate and differentiate. Therefore, the key pathological processes of tumors develop, including vascular sclerosis and chronic inflammation. Indeed, angiogenesis is a complicated process due to various microenvironmental factors, especially with TAMs. Thus, the role of endothelial cells in cervical cancer needs further exploration.

Cytoskeleton associated protein 2 (CKAP2), also known as lamin B1, is a microtubule protein that has microtubule stability and plays a role in controlling cell division. Our previous research has proved that the expression of CKAP2 was significantly upregulated in cervical cancer tissues and correlated with the FIGO staging, lymph node metastasis, recurrence and tumor size. In addition, CKAP2 could participate in cervical cancer proliferation and metastasis through FAK-ERK signaling [4]. However, the impact of CKAP2 on the TME, its relationship with inflammatory cells or endothelial cells in cervical cancer and the underlying mechanism remain unclear.

In the present study, we demonstrated that CKAP2 could regulate the proliferation of endothelial cells in the TME and promote cancer progression with the help of TAMs. Notably, we propose a novel mechanism underlying CKAP2-induced cervical cancer progression through the modulation of the TME via NF-κB signaling.

Materials and methods

Patient sample collection

This study was approved by the ethics committee of the Obstetrics and Gynecology Hospital of Fudan University in accordance with the Helsinki Declaration. Human samples were obtained from the tissue bank of the hospital with written consent, and in total, 64 patient samples (31 from individuals with normal cervices and 33 from patients with cervical squamous cell carcinoma (CSCC)) were collected.

Immunohistochemistry (IHC)

After deparaffinization, dehydration and antigen retrieval, the human and animal tissue slides were immersed in hydrogen peroxide for 15 min and then blocked in goat serum for 1 h. Then, the slides were then incubated overnight at 4°C with the primary antibodies against CD31 (GB11063-2, 1:500) and CD163 (ab18-2422, 1:400). Goat anti-mouse or rabbit secondary antibody (Jiehao, Shanghai) was applied for 1 h at room temperature. The sections were then stained with DAB at room temperature, lightly counterstained with hematoxylin, dehydrated and covered with glass cover slips. Quantification was performed by Image Pro-Plus 6.0, and 3-5 fields were selected to determine the mean optical density (MOD).

Cell culture

Five cervical cancer cell lines (HeLa, SiHa, C-33a, Caski and MS751), THP-1 (human Myeloid Leukemia Mononuclear Cells) and HUVEC (human umbilical vein endothelial cells) were all obtained from the Cell Bank of Academia Sinica (Shanghai, China) and used in this study. HeLa, SiHa, C-33A, Caski, MS751 and THP-1 cells were maintained in RPMI with 10% fetal bovine serum (FBS), 100 units/ml penicillin, 100 μg/ml streptomycin and 0.025 μg/ml amphotericin B and incubated at 37°C with 5% CO_2. HUVECs were cultured in F12 supplemented with 10% fetal bovine serum (FBS), 100 units/ml penicillin, 100 μg/ml streptomycin and 0.025 μg/ml amphotericin B. Lentiviruses were purchased (GeneChem, Shanghai) and used to generate stable CKAP2 (hU6-MCS-Ubiquitin-EGFP-IRES-puromycin) knockdown (kd) and CKAP2 (Ubi-MCS-3FLAG-CBh-gcGFP-IRES-puromycin)-overexpressing (oe) cell lines. CKAP2 was cloned from shRNAs. The MOIs of the cell transduction of kd and oe CKAP2 were both 10.

Reverse transcription-quantitative polymerase chain reaction (RT-PCR)

Cell plates were prepared using TRIzol reagent (Invitrogen). Following the instructions, the mRNA purity and concentration of RNA were identified, and then, 20 μg were reverse transcribed to cDNA. RT-PCR using 384-well optical plates was performed in a SYBR green format with 10 μl template. The following primers were used: primer sequences of CKAP2 forward: 5'-GCCCAAAGAAACCTCGGAAG-3', and reverse: 5'-GCAGGCTCATGCTGAGTAAC-3'. And GAPDH forward: 5'-GCACCGTCAAGGCTGAGAAC-3', and reverse: 5'-TGGTGAAGACGCCAGTGGA-3'. The experiment was repeated 3 times. We used the $2^{-\Delta\Delta CT}$ method to analyse the relative gene

expression. The experiments were replicated 3 times.

Scratch assay

Cell migration was evaluated by a scratch assay. In total, 5×10^5 cancer cells were seeded on a 12-well plate and incubated at 37°C with 5% CO_2. After 8 hours of serum-free incubation, a scratch was made using a 200 μl pipette tip. Photos were taken using an Olympus camera immediately. Twenty-four hours later, photos were taken again by the same equipment. Cell migration was calculated as a percentage of the scratch by ImageJ software. The experiments were replicated 3 times.

Transwell invasion assay

The invasion assay was performed using a Transwell chamber based on the manufacturer's protocol. Cells were trypsinized, washed, and suspended in 50 μl serum-free RPMI with 3×10^4/24 wells. Matrigel was diluted 8-fold and filled in the upper chambers (Corning, America), and RPMI with 20% FBS was added to the lower wells of the chambers. Then, the plate was placed in a 37°C incubator for 24 h. Next, the cells attached to the lower surface were washed with PBS, fixed in 4% paraformaldehyde and stained with 5% crystal violet for 30 min. Images of the cells were captured, and the cell numbers were counted under a microscope at a magnification of × 400. The experiments were replicated 3 times.

CC secreted conditioned medium (CM) and cancer plus THP-1 CM collection

HeLa, SiHa, negative control (nc)-HeLa, kd-HeLa, nc-SiHa and oe-SiHa cells were seeded in complete RPMI in 6-well plates at 1×10^5 cells per 1 mL on the first day, washed with PBS and cultured in serum-free medium the next day for 48 h. Then the cancer CM was collected, centrifuged to eliminate debris and used fresh in the subsequent experiments.

As for cancer plus THP-1 CM collection, we applied two ways of getting CMs. First, cancer/THP-1 CM way. The THP-1 cells were seeded onto 6-well plates at 1×10^6 cells per 1 mL of CM (RPMI containing 100 ng/ml PMA). On the following day, half of the former collection of cancer CM and half of the fresh complete RPMI-cultured macrophages were incubated together for the next 48 h, centrifuged eliminate debris and used fresh in the subsequent HUVEC experiments. Second, cancer/THP-1 coculture CM way. Cancer/THP-1 co CM was constructed by coculturing cancer cells (1×10^5 cells per 1 mL) and macrophages (1×10^6 cells per 1 mL) in a 6-Transwell plate just for 48 h, centrifuging to eliminate debris and used fresh in the subsequent HUVEC experiments.

Flow cytometry

Macrophages were trypsinized, washed and stained for HLA-DR-PE/Cy7 (BioLegend 3076-16), CD86-BV421 (BioLegend 305425), CD-163-APC (BioLegend 333610), and CD206-PE (BioLegend 321106). After 30 min of incubation at room temperature in the dark, the cells were washed twice and resuspended in 300 μl of staining buffer. The cells were analyzed using a Beckman Coulter flow cytometer and FlowJo 10. The experiments were replicated 3 times.

Western blotting analysis

Cells were lysed using radioimmunoprecipitation (RIPA) lysis buffer (Beyotime Biotechnology). After heating at 95°C for 5 min, the samples were separated via SDS-PAGE and electroblotted onto a polyvinylidene difluoride membrane (PVDF) membrane. After blocking with 5% milk, the membrane was incubated with CKAP2 (Santa Cruz, sc-398286, 1:1000), NF-κB p65 (Cell Signaling Technology, CST 6956S, 1:1000), p-NF-κB p65 (CST 3033S, 1:1000), IKKα (CST 11930S, 1:1000), IKKβ (CST 2370S, 1:1000), p-IKKα/β (CST 2078S, 1:1000), IkBα (CST 4812S, 1:1000) and p-IkBα (CST 2859S, 1:1000) overnight at 4°C and then were incubated with HRP-conjugated anti-rabbit/mouse IgG for 1 h at room temperature. The immunoreactive bands were detected by a chemiluminescence system and analyzed using ImageJ. The experiments were replicated 3 times. The experiments were replicated 3 times.

Animal model

BALB/c athymic female nude mice aged 4-6 weeks weighing 20-22 g, were purchased from Slac Laboratory Animal Co., Ltd. (Shanghai, China). The mice were fed in an SPF room in accordance with the institutional guidelines. In

total, 5×10^6 cells/50 μL were subcutaneously injected into the right flank. Twenty mice were divided into the HeLa, SiHa, nc-HeLa, kd-HeLa, nc-SiHa and oe-SiHa groups. The weight and tumor volume were evaluated every 3 days. After 21 or 28 days, all mice were euthanized, and the tumors were collected. The experiments were performed after receiving prior approval by the Institutional Animal Care and Use Committee of Fudan University.

Cell counting kit-8 (CCK-8) proliferation assay

As for HUVECs, HeLa, SiHa, nc-HeLa, kd-HeLa, nc-SiHa, oe-SiHa cells/THP-1 CM were collected. HUVECs were seeded in complete RPMI with 10% FBS in 96-well plates at 1000 cells/well at the first day. On the following day, half of the cancer/THP-1 CM and half of the fresh RPMI with 10% FBS or half of the cancer/THP-1 co CM and half of the fresh RPMI with 10% FBS were added to treat HUVECs. The cell viability was then determined by testing the optical absorbance (450 nm) using a 96-well plate reader at the indicated time points. The experiments were replicated 3 times.

Tube formation

50 μl of ice-cold Matrigel solution (BD sciences) were added into a 96-well plate and incubated at 37°C for 30 min to solidify the gel. HUVECs were suspended in half prepared cancer/THP-1 CM and half fresh F12 medium with 10% FBS or half prepared cancer/THP-1 co CM and half fresh F12 medium with 10% FBS and plated at 3×10^4 cells/well. Images were captured at 6 h and the number of branch nodes and tube circles were measured using ImageJ. The experiments were replicated 3 times.

Confocal microscopy

HUVECs were treated with different CMs, sequentially washed with PBS, and then fixed with 4% paraformaldehyde for 15 min and blocked with goat serum. The samples were incubated with mouse anti-human F-actin (ab205, 1:1000) and rabbit anti-human VE-cadherin (vascular endothelial cadherin junctional index) (ab33168, 1:1000) were incubated at 4°C overnight. F-actin was used to detect the cytoskeleton; thus, the immunofluorescence density of F-actin could be a contrast for VE-cadherin. And VE-cadherin is a classic endothelial adhesion molecule located at junctions between endothelial cells. The cells were incubated with the relevant rabbit or mouse secondary antibodies for 1 h at room temperature. After DAPI staining (Yisheng BioScience, Shanghai), immunofluorescence images were captured under laser scanning confocal microscope (Leica TCS SP5 confocal microscope, Solms, Germany).

Bioinformatics

mRNA transcriptome data were acquired from GEPIA (http://gepia.cancer-pku.cn/) and TCGA (http://portal.gdc.cancer.gov/). Cervical cancer patient clinical characteristics, survival time and follow-up were also acquired; finally, the study included 205 CC samples. CIBERSORT was used to quantify 22 types of human immune cells. Hierarchical agglomerative clustering and unsupervised clustering methods were used to identify different TME cell infiltration patterns in CC. After the TME clusters were constructed, we used differentially expressed genes (DEGs) and R packages for further analysis of the relationship between the TME and clinical and immune cells. As the connection between CKAP2 and immune cell were analyzed using R package.

Statistical analysis

The data analysis was carried out using SPSS 22 and version 3.2.3 of the R software. Chi-square or Fisher's exact test, Wilcoxon rank-sum test and t test were used to analyze the variables. $P < 0.05$ was defined as statistically significant. The data are presented as the means ± SEM.

Results

CKAP2 affects cervical cancer invasion and metastasis

First, we did a bioinformatic analysis of CKAP2 expression in CC from TCGA database. The result turned out that high CKAP2 expression predicted poor overall survival in cervical cancer. Besides, cervical cancer expressed higher CKAP2 level than normal tissues (**Figure 1A**). Next, we detected the expression of CKAP2 in cervical cancer cell lines, including HeLa,

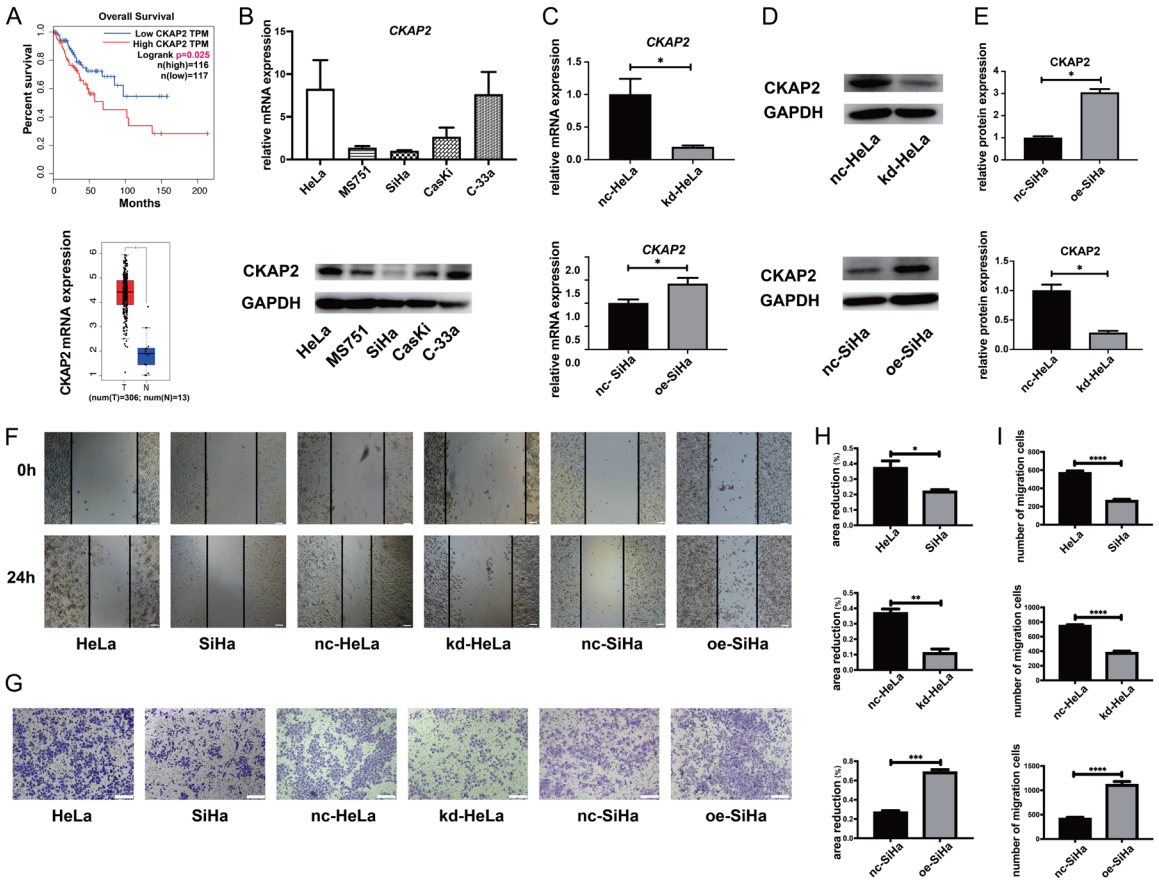

Figure 1. Effect of CKAP2 on cervical cancer invasion and migration. A. The analysis of CKAP2 expression in cervical cancer of TCGA database. B. The expression of CKAP2 in HeLa, MS751, SiHa, CasKi and C-33a cells, five human cervical cancer cell lines, was assessed by RT-PCR and western blot assays. C. The successful knockdown of CKAP2 mRNA expression in HeLa (nc/kd-HeLa) cells and overexpression of CKAP2 in SiHa (nc/oe-SiHa) cells were confirmed by RT-PCR. D. The successful knockdown of CKAP2 protein expression in HeLa (nc/kd-HeLa) cells and the overexpression of CKAP2 in SiHa (nc/oe-SiHa) cells were confirmed by a western blot analysis. E. The successful knockdown of CKAP2 protein expression in HeLa (nc/kd-HeLa) cells and the overexpression of CKAP2 in SiHa (nc/oe-SiHa) cells were measured by quantification of western blot analysis using ImageJ. F. The migration of HeLa, SiHa, nc-HeLa, kd-HeLa, nc-SiHa and oe-SiHa cells was assessed by scratch assays. After the scratch was made for 24 hours, photos were taken. Scale bar = 100 μm. G. The invasion of HeLa, SiHa, nc-HeLa, kd-HeLa, nc-SiHa and oe-SiHa cells was assessed by Transwell assays. After 24 hours, the plates were trypsinized and photographed. Scale bar = 100 μm. H, I. The migration and invasion abilities were measured by quantification of scratch and Transwell assays using ImageJ. Mean ± SEM, t-test. $^{*}P < 0.05$, $^{**}P < 0.01$, $^{***}P < 0.001$, $^{****}P < 0.0001$.

MS751, SiHa, CaSki and C-33a, at both the mRNA and protein levels. The HeLa and C-33a cells showed the highest CKAP2 expression, and the SiHa cells expressed the lowest CKAP2 level (**Figure 1B**). Subsequently, CKAP2 transfected cell lines were successfully established in HeLa and SiHa cells (**Figure 1C-E**), as well as in C-33a cells (Figure S1). But C-33a was hard to be stably passaged (only 5 passages for most), and the transwell assay failed to present stable results. Therefore, we added an intrinsic high/low CKAP2 HeLa/SiHa group. Both the scratch and invasion assay results proved that the high-CKAP2 HeLa cells showed more metastatic characteristics than the low-CKAP2 SiHa cells. Similarly, the scratch and invasion assay experiments using CKAP2 kd-HeLa and CKAP2 oe-SiHa cells suggested that CKAP2 enhanced cervical cancer migration and invasion in vitro. Collectively, our data revealed that CKAP2 could affect cervical carcinoma migration and invasion (**Figure 1F-I**).

Cervical cancer tissues are enriched with macrophages and blood vessels and its connection with CKAP2

Firstly, in order to explore the relationship between CKAP2 and TME, we did a bioinformatic analysis between CKAP2 expression and immune cells in cervical cancer from TCGA database. The result turned out that CKAP2 expression was significantly related with plasma cells (P = 0.018), neutrophils (P = 0.011) and macrophages M0 (P = 0.023) and M2 (P = 0.029) (**Figure 2A**). Furthermore, we systematically analyze TME and cervical cancer prognosis from TCGA, 205 cervical cancer sample were taken into real analysis. Immune cells in TME were calculated by CIBERSORT and principal component analysis (PCA), uncovered 3 distinct patterns of TME subtype with clinicopathologic features. Among the three clusters, cluster B with highest expression of macrophages possessed the worst Overall Survival (OS) which indicated the potential role of macrophages in tumor progression ($P < 0.0001$, **Figure 2B**, **2C**). Besides, confocal images indicated that CKAP2 and microvessels marker CD31 co-expressed in cervical cancer tissues as well (**Figure 2D**).

As the TME is mainly composed of cancer cells, macrophages and endothelial cells, called "invasive niches". Macrophages and angiogenesis play a possible role in the process of cancer progression. We finally determined the expression of CD163 (normal 0.001112 ± 0.0 vs. cervical cancer 0.007034 ± 0.0, $P < 0.0001$) and CD31 (normal 0.006133 ± 0.006345 vs. cervical cancer 0.01737 ± 0.01638, $P < 0.0001$) in both the normal cervix and cervical cancer specimens. Our results indicated that the TAM marker CD163 and microvessel marker CD31 shared prominent populations in the cervical cancer samples compared with those in the normal cervices (**Figure 2E**-**H**), implying that TAMs and microvessels contribute to cervical cancer malignant progression.

CKAP2 affects TME TAMs differentiation

Furthermore, we speculated regarding the phenomenon of the differentiation of THP-1 in response to various CMs. We explored the macrophages differentiation of the M1 HLA-DR+/CD86+ and the M2 CD163+/CD206+ macrophage population following CKAP2 transfection. Unsurprisingly, CD163+/CD206+ macrophage induction was more efficient with high CKAP2 (**Figure 3A**). And HLA-DR+/CD86+ macrophage induction was more efficient in the kd-HeLa and oe-SiHa groups compared with nc-HeLa and nc-SiHa groups respectively (**Figure 3B**). Overall, these data suggest that cervical cancer cells with high CKAP2 may educate macrophages through cytokine secretion.

CKAP2 promotes the proliferation and angiogenesis of HUVECs through the TME

Since TAMs always support angiogenesis, we further determined whether endothelial cells were proliferated or activated by CKAP2 through TME. We actually applied cancer/THP-1 CM (HeLa/SiHa/THP-1, nc/kd-HeLa/THP-1, nc/oe-SiHa/THP-1) and cancer/THP-1 CM co (HeLa/SiHa/THP-1 co, nc/kd-HeLa/THP-1 co, and nc/oe-SiHa/THP-1 co) to determine the function of endothelial cells. The CCK8 results revealed that the treatment of high-expressed CKAP2 CM better activated HUVECs proliferation, while low-expressed CKAP2 decreased HUVECs proliferation (**Figure 3C**). However, the high CKAP2 expression group also exhibited better angiogenesis than the low CKAP2 expression group through tube formation (**Figure 3D**, **3E**). Tube formation could last 12 hours in the TME. Besides, CCK8 and tube formation results proved that there was no difference between the cancer/THP-1 CM and cancer/THP-1 co CM groups.

In addition, we hypothesized that the cervical cancer TME could regulate vascular permeability. Since abnormal tumor vessel leakiness is characterized by interendothelial gaps, we noticed that more interendothelial gaps existed in the high CKAP2 expression group according to the confocal results, especially in the nc-HeLa and oe-SiHa groups (**Figure 3F**). This finding was accompanied by decreased VE-cadherin and increased F-actin [5]. Altogether, these findings indicate that CKAP2 facilitates angiogenesis and endothelial cell cytoskeletal remodeling in cervical cancer.

CKAP2 activates NF-κB signaling in cervical cancer progression

To explore the exact signaling of CKAP2 in cervical cancer progression, a western blot analysis was performed in HeLa/SiHa, nc/kd-CKAP2

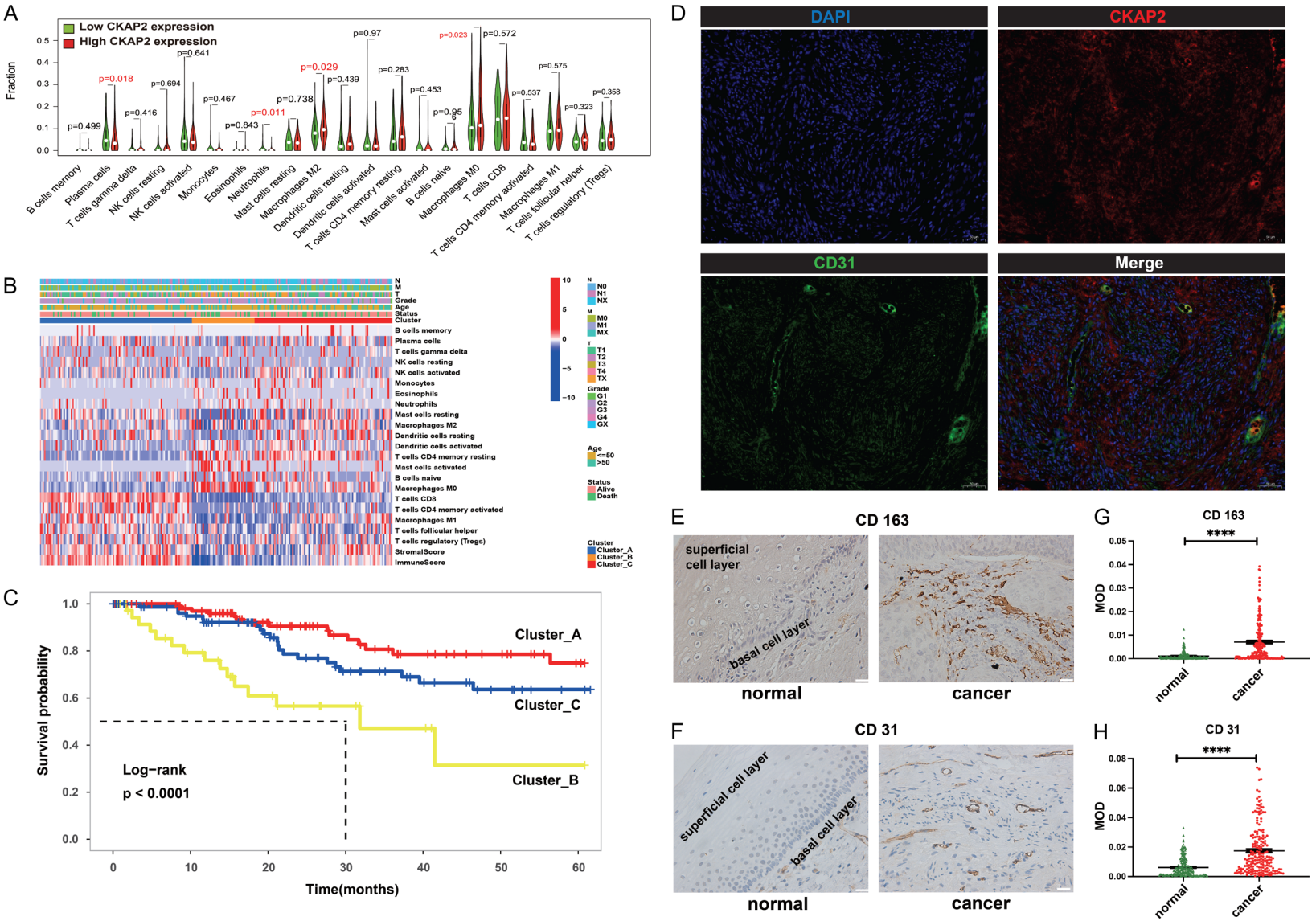

Figure 2. Cervical cancer tissues are enriched with macrophages and microvessels. Normal cervices presented four typical layers, the superficial cell layer, intermediate cell layer, parabasal cell layer and basal cell layer in order. Basal cell layer is easy to recognize, one cell layer with big round nucleus. Superficial cell layer and basal cell layer are labeled in normal picture to view cervical epithelial cell layer and stromal area. A. The fraction of immune cells with high and low CKAP2 expression in cervical cancer. B. The fraction of three TME clusters in cervical cancer. Within each group, the scattered dots represent immune cell expression val-

ues. C. Kaplan-Meier curves of 205 patients showing the association between TME gene clusters and 5-year OS. D. Confocal image of CKAP2 (red), CD31 (green), and DAPI (blue) in cervical cancer tissue. E. Representative IHC brown staining of the TAM marker CD163 in normal and cervical cancer tissues. Scale bar = 50 μm. F. Representative IHC brown staining of the microvessel marker CD31 in normal and cervical cancer tissues. Scale bar = 50 μm. G. IHC MOD comparison evaluation of CD163 between normal and CC tissues. The whole picture is evaluated to quantify MOD. MOD, mean optical density. H. IHC MOD comparison evaluation of CD31 between normal and CC tissues.

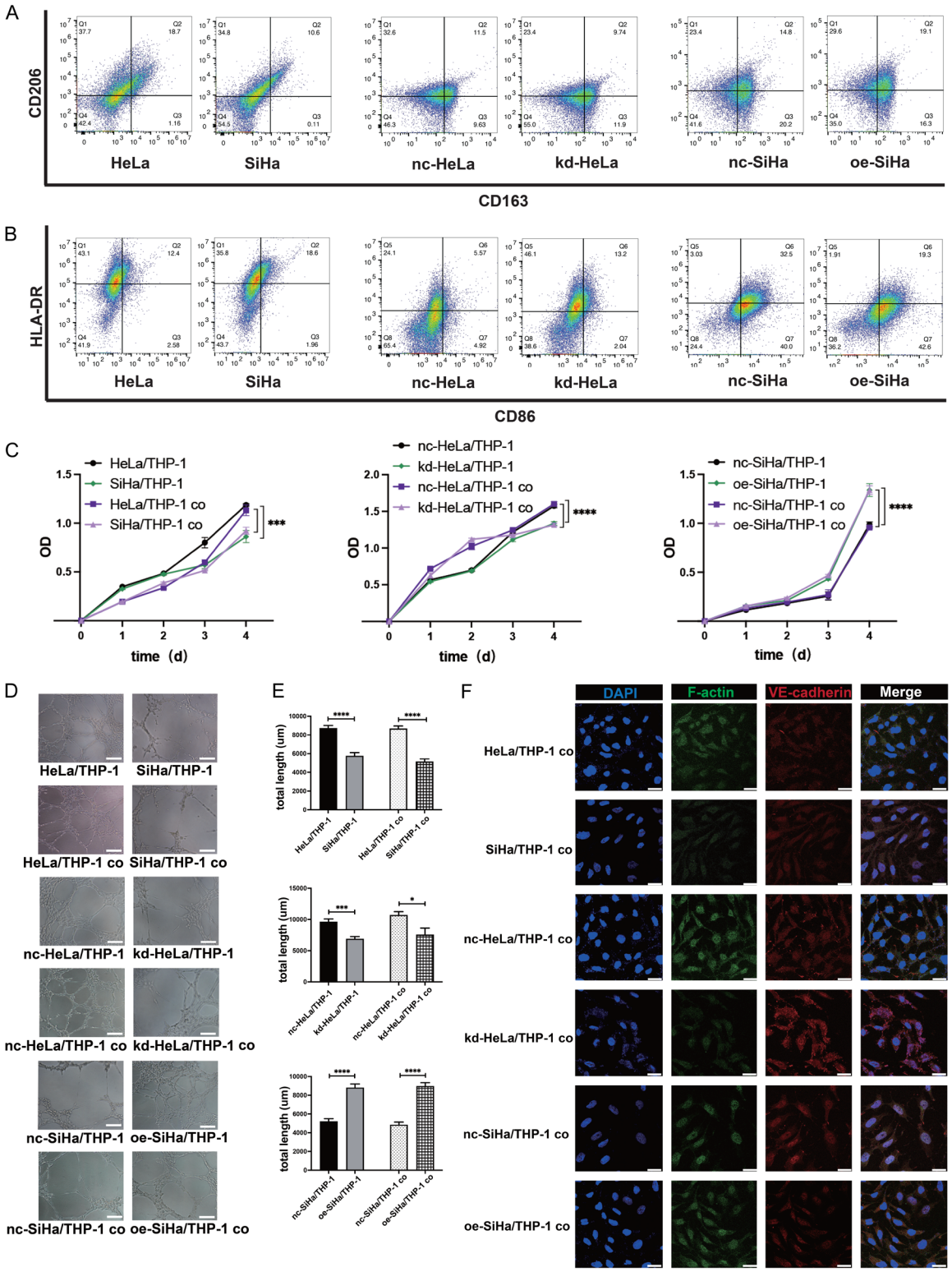

Figure 3. CKAP2 affects the induction of macrophage differentiation, and promotes proliferation and angiogenesis in HUVECs via the TME. A. Fluorescence-activated cell sorting (FACS) dot plots showing CD163+/CD206+ macrophages after the treatment with CM derived from cervical cancer cells. HeLa vs. SiHa, P = 0. 0094; nc-HeLa vs. kd-HeLa, *P* < 0.0001; nc-SiHa vs. oe SiHa, *P* < 0.0001. B. Fluorescence-activated cell sorting (FACS) dot plots showing HLA-DR+/CD86+ macrophages after the treatment with CM derived from cervical cancer cells. HeLa vs. SiHa, P = 0.0498; nc-HeLa vs. kd-HeLa, *P* < 0.0001; nc-SiHa vs. oe SiHa, P = 0.0005. C. A CCK8 proliferation assay was performed with HUVECs. One way, HUVECs were separately treated with HeLa/SiHa/THP-1, nc/kd-HeLa/THP-1, nc/oe-SiHa/THP-1 CM; the other way, HUVECs were separately treated with the HeLa/SiHa/THP-1 co, nc/kd-HeLa/THP-1 co, or nc/oe-SiHa/THP-1 co CM. D. Tube formation was analysed in HUVECs. One way, HUVECs were separately treated with HeLa/SiHa/THP-1, nc/kd-HeLa/THP-1, nc/oe-SiHa/THP-1 CM; and the other way, HUVECs were separately treated with the HeLa/SiHa/THP-1 co, nc/kd-HeLa/THP-1 co, nc/oe-SiHa/THP-1 co CM. Scale bar = 100 μm. E. Tube formation by HUVECs was evaluated. F. Treatment of HUVECs with the HeLa/SiHa/THP-1 co, nc/kd-HeLa/THP-1 co, or nc/oe-SiHa/THP-1 co CM. The "interendothelial gaps" were marked by white lines. Confocal images of F-actin (green), VE-cadherin (red), and DAPI (blue) immunostaining. Scale bar = 25 μm.

HeLa, and nc/oe-CKAP2 SiHa cells. Given that NF-κB is one of the most important transcription factors known to regulate TME inflammation and cancer proliferation and angiogenesis [6], we speculated whether NF-κB signaling factors such as p65, IKKα/β and IκBα and their phosphorylation levels fluctuate with CKAP2. As expected, we found that CKAP2 could activate p-p65, p-IKKα, p-IKKβ and p-IκBα in the HeLa/SiHa, and nc/oe-CKAP2 SiHa groups. The results were the opposite in the nc/kd-CKAP2 group (**Figure 4A**, **4B**). Naturally, it seems that NF-κB signaling was activated in cervical cancer cells.

Subsequently, we evaluated whether NF-κB and IKKα/β inhibitors could prevent this signaling. We applied the signaling inhibitor JSH-23 at concentrations of 10, 30 and 100 nM to block NF-κB signaling in oe-CKAP2 SiHa cells. Luckily, we found that NF-κB signaling protein expression decreased after the treatment with JSH-23, particularly at a concentration of 100 nM after 12 h (**Figure 4C**, **4D**). That is to say, JSH-23 could inhibit the activation of CKAP2 induced NF-κB signaling.

Thereafter, we performed flow cytometry, CCK-8 proliferation, tube formation and confocal to further detect the effect of NF-κB inhibitor in CKAP2 induced TME. Flow cytometry proved that JSH-23 could reverse the induction of macrophages M2 to M1 in high CKAP2 expression of oe-SiHa group with respect to nc-SiHa group level (**Figure 5A**, **5B**). The CCK8 results revealed that the treatment of JSH-23 could obviously suppress HUVECs viability to a very low level induced by oe-SiHa/THP-1 co CM group, even drastically lower than nc-SiHa/THP-1 co CM group (**Figure 5C**). Besides, it could also inhibit the tube formation back to nc-SiHa/THP-1co CM group level when added in oe-SiHa/THP-1 co CM group. And we speculated that even HUVECs gathered, but failed to form branches in i + oe-SiHa/THP-1 co CM group (**Figure 5D**, **5E**). In addition, we noticed increased VE-cadherin and decreased F-actin reoccurred in i + oe-SiHa/THP-1 co CM group (**Figure 5F**). These results suggest that CAKP2 may promote CC progression by modulating TME via NF-κB signaling.

CKAP2 promotes macrophage recruitment and blood vessel formation in vivo

To explore whether CKAP2 expression affects tumorigenesis in vivo, tumor xenografts mice were successfully established. HeLa, SiHa, nc-HeLa, kd-HeLa, nc-SiHa and oe-SiHa cells were injected into the right flanks of nude mice. As shown in **Figure 6**, intrinsic high CKAP2 HeLa cells significantly promoted tumor growth compared with the SiHa cells. The tumors in the HeLa-xenograft mice were larger in volume, heavier in weight and harder to the touch than those of the SiHa-xenograft mice. Furthermore, in the kd-HeLa-xenograft mice, tumor growth and weight were inhibited compared with that in the nc-HeLa-xenograft mice. The average tumor volume in the kd-HeLa-xenograft mouse group was 1000 mm^3 compared with 1500 mm^3 in the nc-HeLa-xenograft mouse group. At the same time, oe-SiHa cells significantly promoted tumor growth compared with nc-SiHa cells. The tumor volume in the oe-SiHa-xenograft mice were larger in volume and heavier in weight than those of the nc-SiHa-xenograft mice (**Figure 6A**, **6D**, **6E**). Then, we conducted CD163 and CD31 staining to determine macrophages and angiogenesis in CKAP2-induced cervical tumor progression. The IHC results

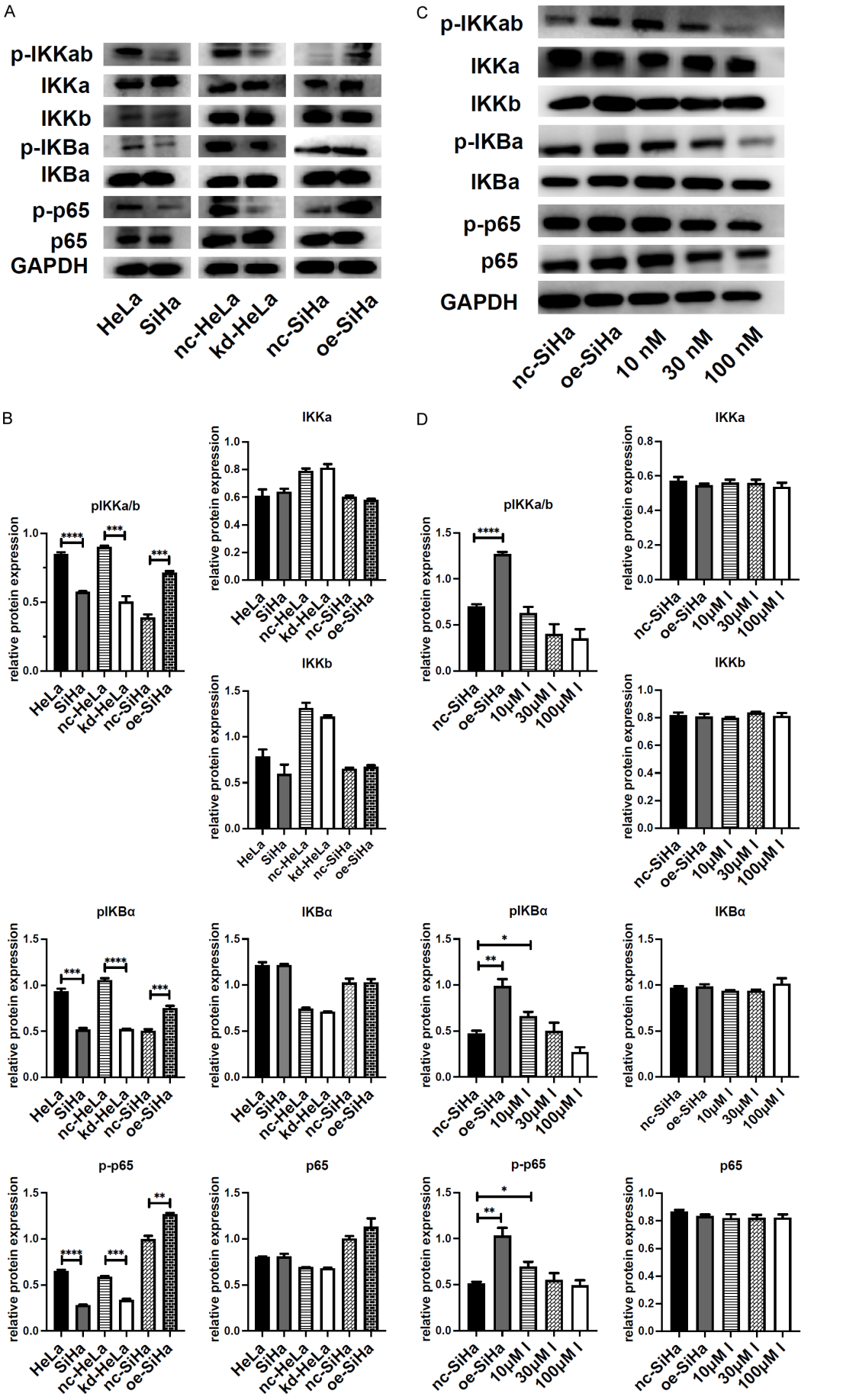
A
p-IKKab
IKKa
IKKb
p-IKBa
IKBa
p-p65
p65
GAPDH
HeLa
SiHa
nc-HeLa
kd-HeLa
nc-SiHa
oe-SiHa
C
p-IKKab
IKKa
IKKb
p-IKBa
IKBa
p-p65
p65
GAPDH
nc-SiHa
oe-SiHa
10 nM
30 nM
100 nM
B
pIKKa/b
IKKa
IKKb
pIKBα
IKBα
p-p65
p65
relative protein expression
D
pIKKa/b
IKKa
IKKb
pIKBα
IKBα
p-p65
p65
relative protein expression
nc-SiHa
oe-SiHa
10μM I
30μM I
100μM I

Figure 4. CKAP2 affects cervical cancer cell cytokine secretion and activates NF-κB signaling in CC. A. The WB image of the NF-κB signaling-associated markers, p65, IKKα/β and IkBα and their phosphorylation levels in HeLa, SiHa, nc-HeLa, kd-HeLa, nc-SiHa and oe-SiHa cells. B. WB image of the NF-κB signaling-associated markers, p65, IKKα/β and IkBα and their phosphorylation levels in nc-SiHa, oe-SiHa, and oe-SiHa cells treated with 10 nM JSH-23 inhibitor, oe-SiHa cells treated with 30 nM JSH-23 inhibitor and oe-SiHa cells treated with 100 nM JSH-23 inhibitor. C. Quantification of the NF-κB signaling-associated markers, p65, IKKα/β and IkBα and their phosphorylation levels in HeLa, SiHa, nc-HeLa, kd-HeLa, nc-SiHa and oe-SiHa cells. D. Quantification of the NF-κB signaling-associated markers, p65, IKKα/β and IkBα and their phosphorylation levels in nc-SiHa, oe-SiHa, and oe-SiHa cells treated with 10 nM JSH-23 inhibitor, oe-SiHa cells treated with 30 nM JSH-23 inhibitor and oe-SiHa cells treated with 100 nM JSH-23 inhibitor.

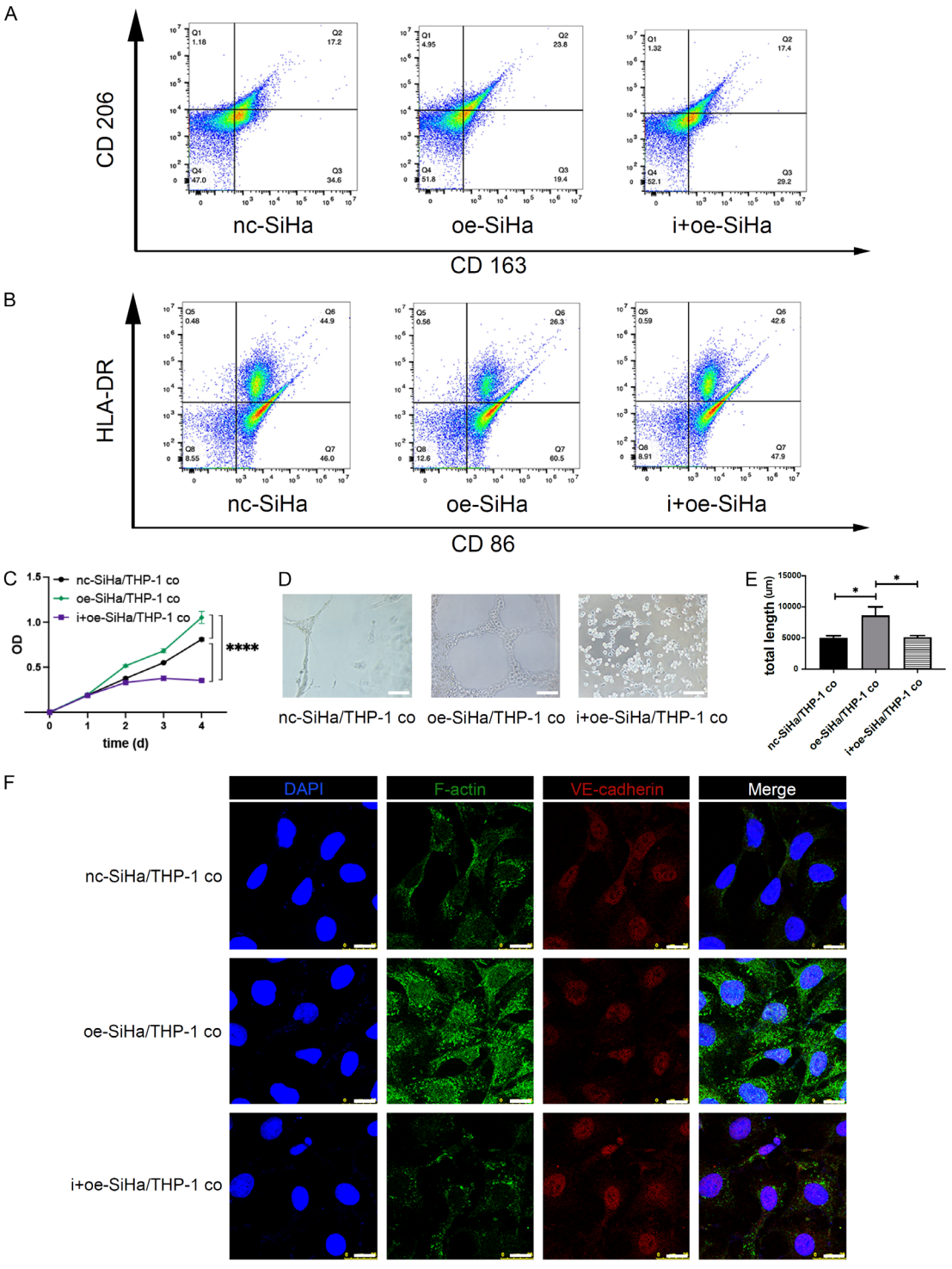

Figure 5. NF-κB inhibitor JSH-23 blocks CKAP2 regulated cervical cancer progression in TME. A. Fluorescence-activated cell sorting (FACS) dot plots showing CD163+/CD206+ macrophages after the treatment with CM derived from nc-SiHa, oe-SiHa and i + oe-SiHa CM, P = 0.0002. B. Fluorescence-activated cell sorting (FACS) dot plots showing HLA-DR+/CD86+ macrophages after the treatment with CM derived from nc-SiHa, oe-SiHa and i + oe-SiHa CM, $P < 0.0001$. C. CCK8 proliferation assay was performed with HUVECs. nc-SiHa/THP-1 co, oe-SiHa/THP-1 co and i + oe-SiHa/THP-1 co CM were collected for treatment. D. Tube formation was analysed in HUVECs. nc-SiHa/THP-1 co, oe-SiHa/THP-1 co and i + oe-SiHa/THP-1 co CM were collected for treatment. Scale bar = 100 μm. E. Tube formation by HUVECs was evaluated. F. Treatment of HUVECs with nc-SiHa/THP-1 co, oe-SiHa/THP-1 co and i + oe-SiHa/THP-1 co CM. Confocal images of F-actin (green), VE-cadherin (red), and DAPI (blue) immunostaining. Scale bar = 25 μm.

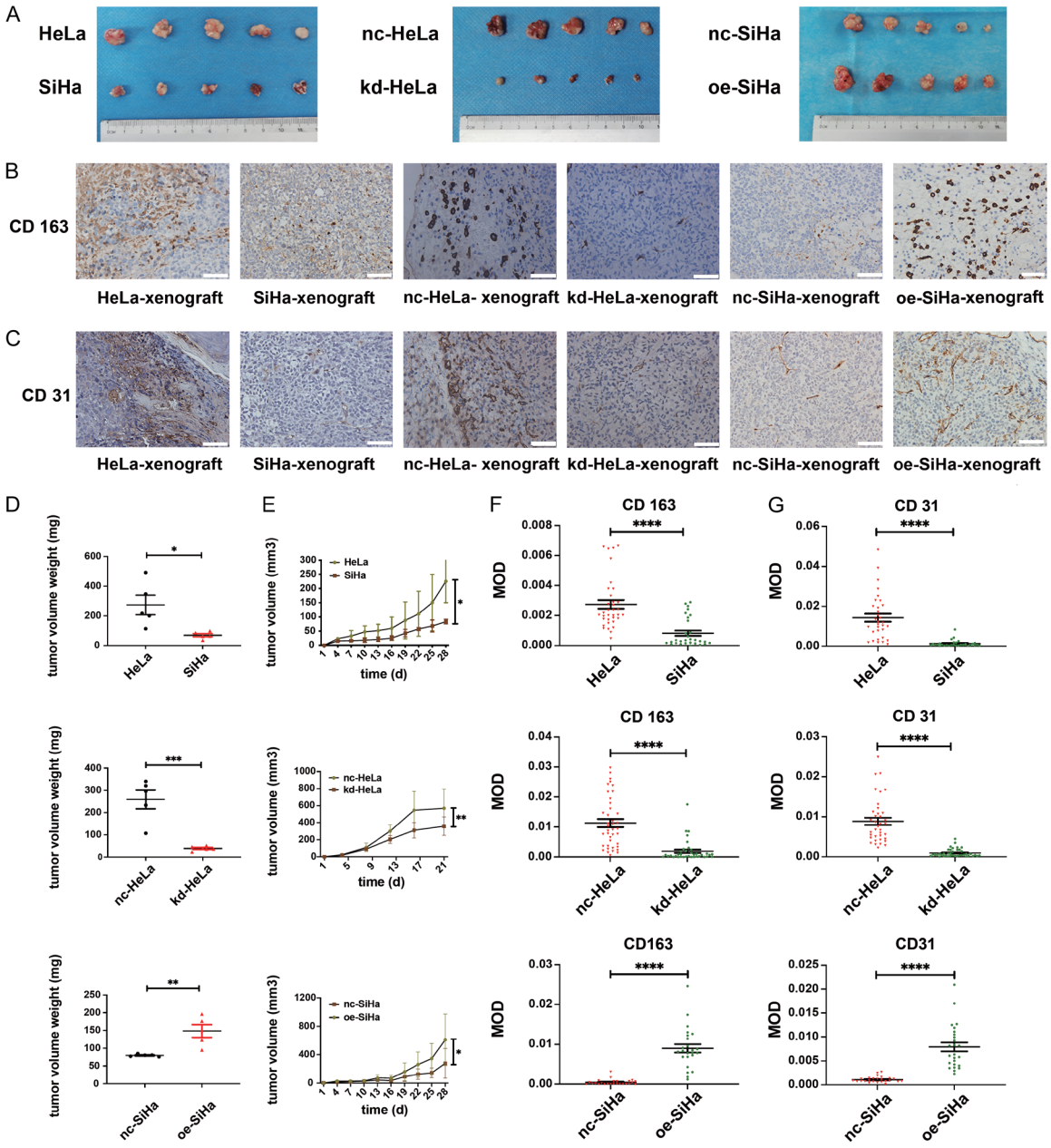

Figure 6. CKAP2 affects macrophage recruitment and blood vessel formation in vivo. A. Pictures of xenografts tumor isolated in 6 groups (HeLa, SiHa, nc-HeLa, kd-HeLa, nc-SiHa and oe-SiHa). B. In vivo TAMs were assessed by CD163 IHC staining. C. In vivo angiogenesis was assessed by CD31 IHC staining. D. The tumor weight of mice in 6 groups (HeLa, SiHa, nc-HeLa, kd-HeLa, nc-SiHa and oe-SiHa) were determined. E. The tumor volume of mice in 6 groups (HeLa, SiHa, nc-HeLa, kd-HeLa, nc-SiHa and oe-SiHa) were determined. F. Immunohistochemistry analysis of the CD163 protein levels in xenograft tumor tissues is shown. G. Immunohistochemistry analysis of the CD31 protein levels in xenograft tumor tissues is shown. Scale bar = 50 μm.

revealed that CKAP2 promoted macrophage recruitment and that CD163 was abundantly expressed in the high CKAP2 mouse groups compared with that in the low CKAP2 groups. In addition, the CD163 staining was mostly located in the tumor stromal area that surrounded tumor cells, which was more obvious in the CKAP2-overexpressing groups. The tendency of the CD31 staining presented similar results, but microvessles were scattered among the entire tumor tissues (**Figure 6B**, **6C**, **6F**, **6G**). Overall, we concluded that CKAP2 could affect monocyte recruitment and blood vessel formation in vivo.

Discussion

With the application of HPV and cytology screening systems, the mortality and morbidity of cervical cancer have been gradually decreasing. However, cervical cancer is still a great burden both mentally and physically worldwide. Currently, cancer recurrence and metastasis are major challenges that lead to death. Our previous research has proved that CKAP2 could promote tumor progression via FAK/ERK signaling in cervical cancer. In this study, we explored the role of CKAP2 in TME inflammation and angiogenesis. We proved that CKAP2 could promote cervical cancer progression by modulating the TME. And we suspected that CKAP2 may influence the process via the inflammation associated pathway NF-κB signaling.

Some researchers have reported that CKAP2 has microtubule-stabilizing properties and plays an important role in the regulation of aneuploidy, the cell cycle, apoptosis and cellular senescence in a p53/TP53-dependent manner [7]. Under normal conditions, CKAP2 expression decreases with cellular senescence and proliferation. Silencing CKAP2 slows cell proliferation and induces premature cellular senescence, while overexpressing CKAP2 increases the proliferation rate and delays cellular senescence [8]. Moreover, other studies have also proven that CKAP2 recruits proinflammatory factors and affects TME homeostasis [9].

Actually, the TME consists of immune cells, fibroblasts, the extracellular matrix and endothelial cells, etc. Specifically, the TME is crucial for regulating immune escape, cancer progression and angiogenesis. Increasing evidence has proved that the TME is not only the final state of cancer development but also initiates cancer progression. Therefore, we investigated the influence of macrophages in cervical cancer. TAMs are among of the most abundant stromal cells in cervical cancer and originate from monocytes. There are two different types of macrophages, namely, classic antitumor M1 macrophages and alternative protumor M2 macrophages. A study showed that when cervical cancer cells and THP-1 were cocultured, the M2 macrophage percentage was elevated with immunosuppressive features [10]. As TAMs tend to share more characteristics of the M2 phenotype, we evaluated the M2 markers CD163 and CD206. The results of both the human and animal studies suggest that TAMs increased with cancer development. Furthermore, our cancer CM culture experiment showed that the tendency of M2 differentiation was more evident with CAKP2 expression while M1 differentiation got weaker. By the way, an increasing number of scientists have suggested that TAMs are more complex than the classical M1/M2 model [11]. An article even reported that the C1QC+ and SPP1+ TAM gene signatures, but not the M1/M2 signature, could more accurately characterize CC patients [12]. More efforts are needed to explore more valuable potential markers for TAMs. Overall, we regard CKAP2 as the factor mediating the crosstalk between cancer cells and macrophages and promote cancer progression.

The ecosystem of the TME is a complex. Surprisingly, few studies have considered the crosstalk among cervical cancer, macrophages and angiogenesis. To some degree, this study adds some value to this field. In fact, TAMs irrigate endothelial cells and propel angiogenesis [13]. Moreover, when the tumor size exceeds 1 to 2 mm in diameter, angiogenetic factors form an angiogenic network and induce the sprouting of blood vessels [14]. More specifically, CD31 revealed an MVD (microvascular density) increase in CC. VEGF was also enriched in tumor tissues. The CM of CKAP2 cancer/THP-1 cells promoted angiogenesis proliferation. Tube formation indicates blood vessel branch formation. Immunofluorescence presented the vascular permeability. All these results demonstrated that CKAP2 could facilitate cervical

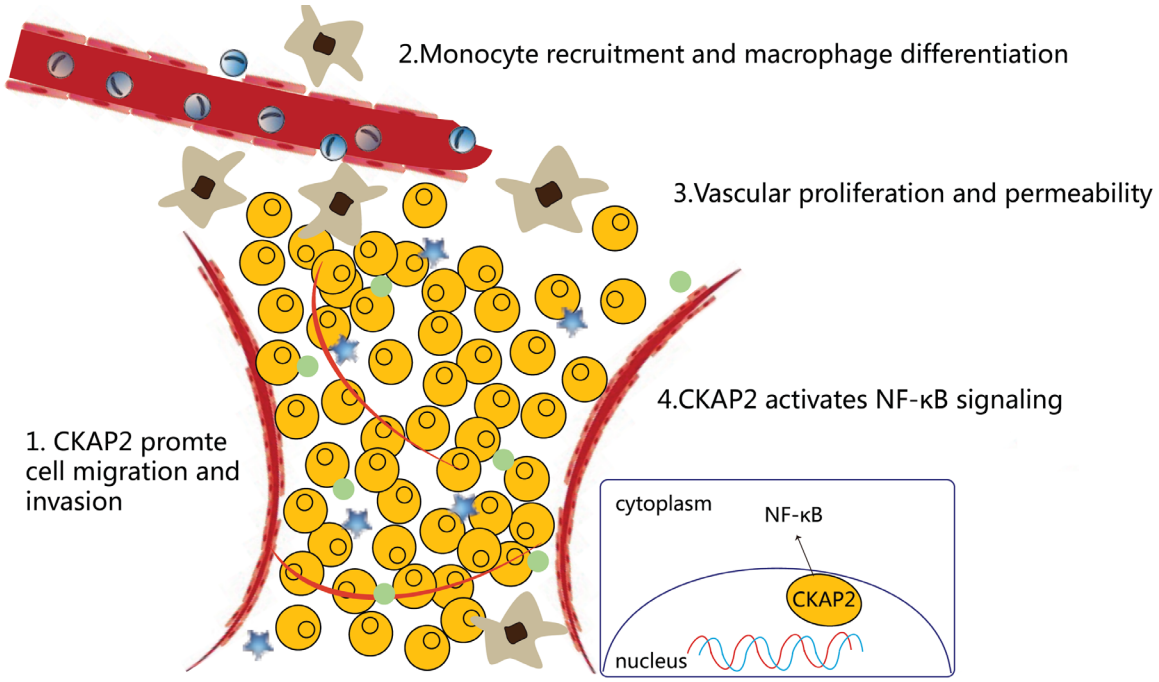

Figure 7. Schematic picture depicting the proposed mechanism of CKAP2 in cervical cancer. CKAP2 could promote cancer cell migration and invasion by modulating TME inflammation and angiogenesis via NF-κB signaling.

cancer by reprogramming microenvironment TAMs and angiogenesis. We could easily understand that the anti-VEGF strategy sometimes has limited efficiency and potential resistance because a single target treatment is not enough to treat the complicated TME. Therefore, modern precision medicine should expand the border of merely cancer cells to TME stromal cells.

In summary, the frequent interactions between cancer cells and TME stromal cells are essential for stimulating tumor heterogeneity and progression. Therefore, by remodeling TME tumor cells and stromal cells, exerting their regurgitation-feeding behavior between TAMs and endothelial cells or other stromal cells could influence cervical cancer progression. Therefore, understanding the underlying cellular and molecular mechanism governing cervical cancer and TME remodeling could contribute to the development of promising therapeutic management [15].

In addition, the NF-κB system is critical for coordinating inflammatory responses, innate and adaptive immunity, cellular differentiation and proliferation, and survival in multicellular organisms [16]. Luckily, we proved that NF-κB signaling is activated during tumor development; moreover, we collected CM from cells treated with NF-κB inhibitor and checked some features for TME, flow cytometry, CCK-8 assay, tube formation, confocal, etc. Thus, we naturally suspected that the classic inflammatory NF-κB signaling pathway may modulate CKAP2 between cervical cancer and stromal cells, reprogramming the TME and generating a positive feedback loop in cancer progression, which needs further exploration.

Although the current work introduces crosstalk among CKAP2, inflammation and angiogenesis and the process may be connected via NF-κB signaling, it has not entirely revealed the iceberg of the mechanism of autocrine and paracrine manner with cytokines or chemokines in this study [17]. Moreover, tumor angiogenesis could occur more specific and persuasive results if we successfully built a macrophage-deleted animal model. In addition, it could be more convincing if larger amounts of human samples were collected.

Meanwhile, hypoxia is a main driver of tumor angiogenesis that activates macrophage M2 and reactive oxygen species (ROS) imbalance. In fact, silencing CKAP2 caused a p53-dependent decrease in mitochondrial ROS accompa-

nied by cell proliferation defects based on a recent report [18]. Precisely, the tumor suppressor gene p53 maintained a tight bond with cervical cancer initiation, and it would be exciting to explore their relationship with the TME in our future research. Moreover, according to our unpublished mass spectrometry results, it is promising to determine the role of associated transcription factors or enzymes, which might enlighten us in determining the mechanism of tumor progression and invasion with CKAP2 better.

Conclusion

CKAP2 promotes cervical cancer progression by modulating TME inflammation and angiogenesis, and CKAP2/NF-κB signaling may exert an irreplaceable function (**Figure 7**). Future challenges will involve in the determination of discovery of effective target medicine and determining the optimal duration treatment, including how to develop effective therapies for metastatic, adjuvant and neoadjuvant cases.

Acknowledgements

This study was supported by the National Natural Science Foundation of China (Grant No. 82173188) to KQ Hua, the Clinical Research Plan of SHDC (SHDC2020CR1045B, SHDC-2020CR6009) to KQ Hua, the Research and Innovation Project of the Shanghai Municipal Education Commission (No. 2019-01-07-00-07-E00050) to KQ Hua, the National Natural Science Foundation of China (Grant No. 819-71361) to JJ Qiu, the Natural Science Foundation of Shanghai Science and Technology (No. 19ZR1406900) to JJ Qiu, the Shanghai 'Rising Stars of Medical Talent' Youth Development Program (No. AB83030002019004) to JJ Qiu, the Clinical Research Plan of SHDC (No. SHDC2020CR4087) to JJ Qiu, Shanghai Municipal Health Commission (No. 202040498) to JJ Qiu.

Disclosure of conflict of interest

None.

Abbreviation

CC, cervical cancer; TME, tumor microenvironment; TAMs, Tumor-associated macrophages; CIN, cervical intraepithelial neoplasia; CM, conditioned medium; CSCC, cervical squamous cell carcinoma; MOD, mean optical density; SASP, senescence-associated secretory phenotype; ROS, reactive oxygen species.

Address correspondence to: Drs. Junjun Qiu and Keqin Hua, Gynecology Oncology Department, Obstetrics and Gynecology Hospital of Fudan University, Shanghai, China. E-mail: qiujunjun1113@163.com (JJQ); huakeqinjiaoshou@163.com (KQH)

References

[1] Hammes LS, Tekmal RR, Naud P, Edelweiss MI, Kirma N, Valente PT, Syrjanen KJ and Cunha-Filho JS. Macrophages, inflammation and risk of cervical intraepithelial neoplasia (CIN) progression-clinicopathological correlation. Gynecol Oncol 2007; 105: 157-165.

[2] Liu Y, Li L, Li Y and Zhao X. Research progress on tumor-associated macrophages and inflammation in cervical cancer. Biomed Res Int 2020; 2020: 6842963.

[3] Pedraza-Brindis EJ, Sanchez-Reyes K, Hernandez-Flores G, Bravo-Cuellar A, Jave-Suarez LF, Aguilar-Lemarroy A, Gomez-Lomeli P, Lopez-Lopez BA and Ortiz-Lazareno PC. Culture supernatants of cervical cancer cells induce an M2 phenotypic profile in THP-1 macrophages. Cell Immunol 2016; 310: 42-52.

[4] Guo QS, Song Y, Hua KQ and Gao SJ. Involvement of FAK-ERK2 signaling pathway in CKAP2-induced proliferation and motility in cervical carcinoma cell lines. Sci Rep 2017; 7: 2117.

[5] Giannotta M, Trani M and Dejana E. VE-cadherin and endothelial adherens junctions: active guardians of vascular integrity. Dev Cell 2013; 26: 441-454.

[6] Yin K, Patten D, Gough S, de Barros Gonçalves S, Chan A, Olan I, Cassidy L, Poblocka M, Zhu H, Lun A, Schuijs M, Young A, Martinez-Jimenez C, Halim TYF, Shetty S, Narita M and Hoare M. Senescence-induced endothelial phenotypes underpin immune-mediated senescence surveillance. Genes Dev 2022; 36: 533-549.

[7] Shimi T, Butin-Israeli V, Adam SA, Hamanaka RB, Goldman AE, Lucas CA, Shumaker DK, Kosak ST, Chandel NS and Goldman RD. The role of nuclear lamin B1 in cell proliferation and senescence. Genes Dev 2011; 25: 2579-2593.

[8] Zhang S, Wang Y, Chen S and Li J. Silencing of cytoskeleton-associated protein 2 represses cell proliferation and induces cell cycle arrest and cell apoptosis in osteosarcoma cells. Biomed Pharmacother 2018; 106: 1396-1403.

[9] Garvalov BK, Muhammad S and Dobreva G. Lamin B1 in cancer and aging. Aging (Albany NY) 2019; 11: 7336-7338.
[10] Jiang S, Yang Y, Fang M, Li X, Yuan X and Yuan J. Co-evolution of tumor-associated macrophages and tumor neo-vessels during cervical cancer invasion. Oncol Lett 2016; 12: 2625-2631.
[11] Zhang Q, He Y, Luo N, Patel SJ, Han Y, Gao R, Modak M, Carotta S, Haslinger C, Kind D, Peet GW, Zhong G, Lu S, Zhu W, Mao Y, Xiao M, Bergmann M, Hu X, Kerkar SP, Vogt AB, Pflanz S, Liu K, Peng J, Ren X and Zhang Z. Landscape and dynamics of single immune cells in hepatocellular carcinoma. Cell 2019; 179: 829-845, e820.
[12] Li X, Zhang Q, Chen G and Luo D. Multi-omics analysis showed the clinical value of gene signatures of C1QC(+) and SPP1(+) TAMs in cervical cancer. Front Immunol 2021; 12: 694801.
[13] Chávez-Galán L, Olleros ML, Vesin D and Garcia I. Much more than M1 and M2 macrophages, there are also CD169(+) and TCR(+) macrophages. Front Immunol 2015; 6: 263.
[14] Wu XG, Zhou CF, Zhang YM, Yan RM, Wei WF, Chen XJ, Yi HY, Liang LJ, Fan LS, Liang L, Wu S and Wang W. Cancer-derived exosomal miR-221-3p promotes angiogenesis by targeting THBS2 in cervical squamous cell carcinoma. Angiogenesis 2019; 22: 397-410.
[15] Georgouli M, Herraiz C, Crosas-Molist E, Fanshawe B, Maiques O, Perdrix A, Pandya P, Rodriguez-Hernandez I, Ilieva KM, Cantelli G, Karagiannis P, Mele S, Lam H, Josephs DH, Matias-Guiu X, Marti RM, Nestle FO, Orgaz JL, Malanchi I, Fruhwirth GO, Karagiannis SN and Sanz-Moreno V. Regional activation of myosin II in cancer cells drives tumor progression via a secretory cross-talk with the immune microenvironment. Cell 2019; 176: 757-774, e723.
[16] Mitchell S, Vargas J and Hoffmann A. Signaling via the NFκB system. Wiley Interdiscip Rev Syst Biol Med 2016; 8: 227-241.
[17] Chen P, Huang Y, Bong R, Ding Y, Song N, Wang X, Song X and Luo Y. Tumor-associated macrophages promote angiogenesis and melanoma growth via adrenomedullin in a paracrine and autocrine manner. Clin Cancer Res 2011; 17: 7230-7239.
[18] Yue S, Zheng X and Zheng Y. Cell-type-specific role of lamin-B1 in thymus development and its inflammation-driven reduction in thymus aging. Aging Cell 2019; 18: e12952.

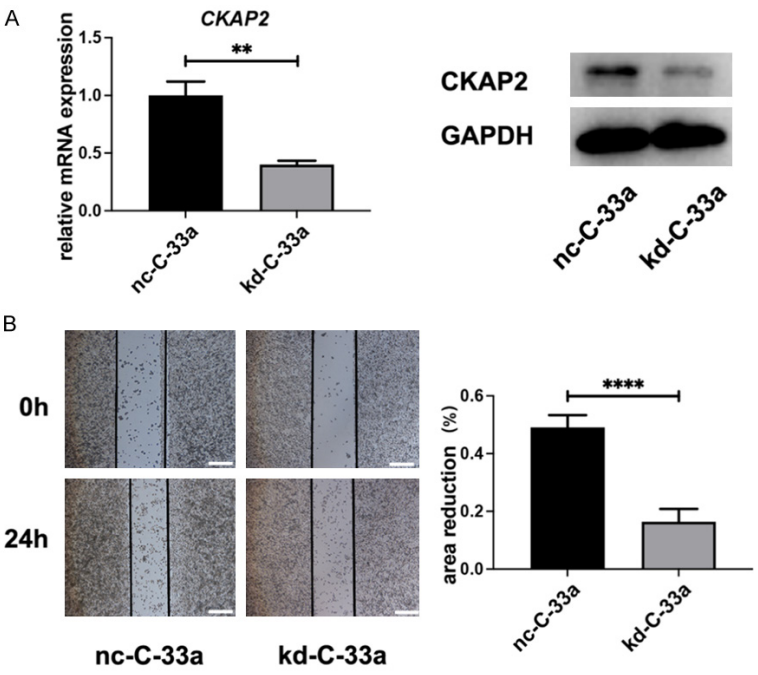

Figure S1. Effect of CKAP2 on C-33a. A. The successful knockdown of CKAP2 mRNA and protein expression in C-33a (nc/kd-C-33a) cells were confirmed by RT-PCR and Western blot. B. The migration of nc/kd-C-33a was assessed by scratch assays. After the scratch was made for 24 hours, photos were taken. Scale bar = 100 μm.